

# Quantum Natural Gradient

James Stokes,<sup>1</sup> Josh Izaac,<sup>2</sup> Nathan Killoran,<sup>2</sup> and Giuseppe Carleo<sup>3</sup>

<sup>1</sup>*Center for Computational Quantum Physics and Center for Computational Mathematics, Flatiron Institute, New York, NY 10010 USA*

<sup>2</sup>*Xanadu, 777 Bay Street, Toronto, Canada*

<sup>3</sup>*Center for Computational Quantum Physics, Flatiron Institute, New York, NY 10010 USA*

(Dated: December 23, 2019)

A quantum generalization of Natural Gradient Descent is presented as part of a general-purpose optimization framework for variational quantum circuits. The optimization dynamics is interpreted as moving in the steepest descent direction with respect to the Quantum Information Geometry, corresponding to the real part of the Quantum Geometric Tensor (QGT), also known as the Fubini-Study metric tensor. An efficient algorithm is presented for computing a block-diagonal approximation to the Fubini-Study metric tensor for parametrized quantum circuits, which may be of independent interest.

## I. INTRODUCTION

Variational optimization of parametrized quantum circuits is an integral component for many hybrid quantum-classical algorithms, which are arguably the most promising applications of Noisy Intermediate-Scale Quantum (NISQ) computers [1]. Applications include the Variational Quantum Eigensolver (VQE) [2], Quantum Approximate Optimization Algorithm (QAOA) [3] and Quantum Neural Networks (QNNs) [4–6].

All the above are examples of stochastic optimization problems whereby one minimizes the expected value of a random cost function over a set of variational parameters, using noisy estimates of the cost and/or its gradient. In the quantum setting these estimates are obtained by repeated measurements of some Hermitian observables for a quantum state which depends on the variational parameters.

A variety of optimization methods have been proposed in the variational quantum circuit literature for determining optimal variational parameters, including derivative-free (zeroth-order) methods such as Nelder-Mead, finite-differencing [7] or SPSA [8]. Recently the possibility of exploiting direct access to first-order gradient information has been explored. Indeed quantum circuits have been designed to estimate such gradients with minimal overhead compared to objective function evaluations [9].

One motivation for exploiting first-order gradients is theoretical: in the convex case, the expected error in the objective function using the best known zeroth-order stochastic optimization algorithm scales polynomially with the dimension  $d$  of the parameter space, whereas Stochastic Gradient Descent (SGD) converges independently of  $d$ . Another motivation stems from the empirical success of stochastic gradient methods in training deep neural networks, which involve minimization of non-convex objective functions over high-dimensional parameter spaces.

The application of SGD to deep learning suffers from the caveat that successful optimization hinges on careful hyper-parameter tuning of the learning rate (step

size) and other hyper-parameters such as Momentum. Indeed a vast literature has developed devoted to step size selection (see e.g. [10]). The difficulty of choosing a step size can be understood intuitively in the simple quadratic bowl approximation, where the optimal step size depends on the maximum eigenvalue of the Hessian, a quantity which is difficult to calculate in high dimensions. In practical applications the step size selection problem is overcome by using adaptive methods of stochastic optimization such as Adam [11] which have enjoyed wide adoption because of their ability to dynamically select a step size by maintaining a history of past gradients.

Independently of the improvements arising from historical averaging as in Momentum and Adam, it is natural to ask if the geometry of quantum states favors a particular optimization strategy. Indeed, it is well-known that the choice of optimization is intimately linked to the choice of geometry on the parameter space [12]. In the most well-known case of vanilla gradient descent, the relevant geometry corresponds to the  $l_2$  geometry as can be seen from the following exact rewriting of the iterative update rule

$$\begin{aligned} \theta_{t+1} &:= \theta_t - \eta \nabla \mathcal{L}(\theta_t) , \\ &= \arg \min_{\theta \in \mathbb{R}^d} \left[ \langle \theta - \theta_t, \nabla \mathcal{L}(\theta_t) \rangle + \frac{1}{2\eta} \|\theta - \theta_t\|_2^2 \right] , \end{aligned} \quad (1)$$

where  $\mathcal{L}$  is the loss as a function of the variational parameters  $\theta \in \mathbb{R}^d$  and  $\eta$  is the step size. Thus, vanilla gradient descent moves in the steepest descent direction with respect to the  $l_2$  geometry.

In the deep learning literature, it has been argued that the  $l_2$  geometry is poorly adapted to the space of weights of deep networks, due to their intrinsic parameter redundancy [12]. The Natural Gradient [13], in contrast, moves in the steepest descent direction with respect to the Information Geometry. This natural gradient descent is advantageous compared to the vanilla gradient because it is invariant under arbitrary re-parametrizations [13] and moreover possesses an approximate invariance with respect to over-parametrizations [14], which are typical for deep neural

networks.

In a similar spirit, the quantum circuit literature has investigated the impact of geometry on dynamics of variational algorithms. In particular, it was shown that under the assumption of strong convexity, the  $l_2$  geometry is sub-optimal in some situations compared to the  $l_1$  geometry [15]. The intuitive argument put forth favoring the  $l_1$  geometry is that some quantum state ansätze can be physically interpreted as a sequence of pulses of Hamiltonian evolution, starting from a fixed reference state. In this particular parametrization, each variational parameter can be interpreted as the duration of the corresponding pulse. This is not the only useful parametrization of quantum states, however, and it is thus desirable to find a descent direction which is not tied to any particular parametrization.

Ref. [15] leaves open the problem of finding the relevant geometry for general-purpose variational quantum algorithms, and this paper seeks to fill that void. The contributions of this papers are as follows:

- We point out that the demand of invariance with respect to arbitrary reparametrizations can be naturally fulfilled by introducing a Riemannian metric tensor on the space of quantum states, and that the implied descent direction is invariant with respect to reparametrizations by construction.
- We note that the space of quantum states is naturally equipped with a Riemannian metric, which differs from  $l_2$  and  $l_1$  geometries explored previously. In fact, in the absence of noise, the space of quantum states is a complex projective space, which possesses a unique unitarily-invariant metric tensor called the Fubini-Study metric tensor. When restricted to the submanifold of quantum states defining the parametric family, the Fubini-Study metric tensor emerges as the real part of a more general geometric quantity called the Quantum Geometric Tensor (QGT).
- We show that the resulting gradient descent algorithm is a direct quantum analogue of the Natural Gradient in the statistics literature, and reduces to it in a certain limit.
- We present quantum circuit construction which computes a block-diagonal approximation to the Quantum Geometric Tensor and show that a simple diagonal preconditioning scheme outperforms vanilla gradient descent in terms of number of iterates required to achieve convergence

## II. THEORY

### A. Quantum Information Geometry

Consider the set of probability distributions on  $N$  elements  $[N] = \{1, \dots, N\}$ ; that is, the set of positive

vectors  $p \in \mathbb{R}^N$ ,  $p \succeq 0$  which are normalized in the 1-norm  $\|p\|_1 = 1$ . The following function is easily shown to be a metric (Fisher-Rao metric) on the probability simplex  $\Delta^{N-1}$ ,

$$d(p, q) = \arccos(\langle \sqrt{p}, \sqrt{q} \rangle) , \quad (2)$$

where  $\sqrt{p}$  and  $\sqrt{q}$  denote the elementwise square root of the probability vectors in the probability simplex  $p, q \in \Delta^{N-1}$ .

Now consider a parametric family of strictly positive probability distributions  $p_\theta \succ 0$  indexed by real parameters  $\theta \in \mathbb{R}^d$ . It can be shown that the infinitesimal squared line element between two members of the parametric family is given by

$$d^2(p_\theta, p_{\theta+d\theta}) = \frac{1}{4} \sum_{(i,j) \in [d]^2} I_{ij}(\theta) d\theta^i d\theta^j , \quad (3)$$

where  $I_{ij}(\theta)$  are the components of a Riemannian metric tensor (with possible degeneracies) called the Fisher Information Matrix. Letting  $p_\theta(x)$  denote the component of the probability vector  $p_\theta$  corresponding to  $x \in [N]$  we have

$$I_{ij}(\theta) = \sum_{x \in [N]} p_\theta(x) \frac{\partial \log p_\theta(x)}{\partial \theta^i} \frac{\partial \log p_\theta(x)}{\partial \theta^j} . \quad (4)$$

Now consider a  $N$ -dimensional complex Hilbert space  $\mathbb{C}^N$ . Given a vector  $\psi \in \mathbb{C}^N$  which is normalized in the 2-norm  $\|\psi\|_2 = 1$ , a pure quantum state is defined as the projection  $P_\psi = |\psi\rangle\langle\psi| \in \mathbb{C}\mathbb{P}^{N-1}$  onto the one-dimensional subspace spanned by the unit vector  $\psi$ . In direct analogy with the simplex, the following function is easily shown to be a metric (Fubini-Study metric) on the space of pure states:

$$d(P_\psi, P_\phi) = \arccos(|\langle\psi, \phi\rangle|) , \quad (5)$$

where  $\psi, \phi \in \mathbb{C}^N$  are unit vectors. Letting  $\psi_\theta$  denote a parametric family of unit vectors, the infinitesimal squared line element between two states defined by the parametric family is given by

$$d^2(P_{\psi_\theta}, P_{\psi_{\theta+d\theta}}) = \sum_{(i,j) \in [d]^2} g_{ij}(\theta) d\theta^i d\theta^j , \quad (6)$$

where  $g_{ij}(\theta) = \text{Re}[G_{ij}(\theta)]$  is the Fubini-Study metric tensor, which can be expressed in terms of the following Quantum Geometric Tensor (see [16] for a review),

$$G_{ij}(\theta) = \left\langle \frac{\partial \psi_\theta}{\partial \theta^i}, \frac{\partial \psi_\theta}{\partial \theta^j} \right\rangle - \left\langle \frac{\partial \psi_\theta}{\partial \theta^i}, \psi_\theta \right\rangle \left\langle \psi_\theta, \frac{\partial \psi_\theta}{\partial \theta^j} \right\rangle . \quad (7)$$

Indeed if  $\{|x\rangle : x \in [N]\}$  denotes an orthonormal basis for  $\mathbb{C}^N$  then one can easily verify that for the family of unit vectors defined by

$$\psi_\theta = \sum_{x \in [N]} \sqrt{p_\theta(x)} |x\rangle , \quad (8)$$

we have  $G_{ij}(\theta) = \frac{1}{4}I_{ij}(\theta)$ .

Finally, although we have posed the discussion in finite-dimensions, all of the above concepts carry over to infinite-dimensional Hilbert spaces by appropriately replacing sums by integrals.

### B. Optimization problem

Consider a parametric family of unitary operators  $U(\theta) \in U(N)$  which are indexed by real parameters  $\theta \in \mathbb{R}^d$ . Given a fixed reference unit vector  $|0\rangle \in \mathbb{C}^N$  and a Hermitian operator  $H = H^\dagger$  acting on  $\mathbb{C}^N$ , we consider the following optimization problem

$$\min_{\theta \in \mathbb{R}^d} \mathcal{L}(\theta) , \quad \mathcal{L}(\theta) = \frac{1}{2} \text{tr}(P_{\psi_\theta} H) = \frac{1}{2} \langle \psi_\theta, H \psi_\theta \rangle , \quad (9)$$

where  $\psi_\theta = U_\theta|0\rangle$  and  $P_{\psi_\theta} \in \mathbb{C}\mathbb{P}^{N-1}$  is the associated projector. In particular, note that  $\psi_\theta$  is normalized since  $U(\theta)$  is unitary. Global optimization of the nonconvex objective function  $\mathcal{L}(\theta)$  is impractical, so we instead propose to search for local optima by iterating the following discrete-time dynamical system,

$$\theta_{t+1} = \arg \min_{\theta \in \mathbb{R}^d} \left[ \langle \theta - \theta_t, \nabla \mathcal{L}(\theta_t) \rangle + \frac{1}{2\eta} \|\theta - \theta_t\|_{g(\theta_t)}^2 \right] , \quad (10)$$

where  $g(\theta_t)$  is the symmetric matrix with  $(i, j)$  component  $\text{Re}[G_{ij}(\theta_t)]$  and we have introduced the following notation:

$$\|\theta - \theta_t\|_{g(\theta_t)}^2 = \langle \theta - \theta_t, g(\theta_t)(\theta - \theta_t) \rangle . \quad (11)$$

The first-order optimality condition corresponding to (10) is

$$g(\theta_t)(\theta_{t+1} - \theta_t) = \eta \nabla \mathcal{L}(\theta_t) , \quad (12)$$

which we solve using the pseudo-inverse  $g^+(\theta_t)$  as follows,

$$\theta_{t+1} = \theta_t - \eta g^+(\theta_t) \nabla \mathcal{L}(\theta_t) . \quad (13)$$

In the continuous-time limit corresponding to vanishing step size  $\eta \rightarrow 0$ , the dynamics (10) is equivalent to imaginary-time evolution within the variational subspace according to the Hamiltonian  $H$ , as shown in the supplementary material.

### C. Relationship with previous work

In the Variational Quantum Monte Carlo literature, the Stochastic Reconfiguration algorithm [17] has been developed which produces a stochastic estimate of (13) by classical sampling from the Born probability distribution corresponding to  $\psi_\theta$ . An associated real-time evolution algorithm, which exploits the the imaginary part  $\text{Im}[G_{ij}(\theta)]$  of the Quantum Geometric Tensor (7)

has been developed in [18] and subsequently demonstrated on quantum hardware in [19]. For details on the geometry of the time-dependent variational principle we refer the reader to [20, Proposition 2.4]. Variational imaginary-time evolution on hybrid quantum-classical devices has been previously investigated in [21–23]. In these works, the choice of optimization geometry can be shown to correspond to the unit sphere  $\mathbb{S}^{N-1} = \{\psi \in \mathbb{C}^N : \|\psi\|_2 = 1\}$ , rather than the complex projective space  $\mathbb{C}\mathbb{P}^{N-1}$  utilized in this paper. Recently, Ref. [24] appeared which considers general evolution of variational density matrices in both real and imaginary time, from a different perspective. By restricting their proposal to pure state projectors (elements of  $\mathbb{C}\mathbb{P}^{N-1}$ ) they find an algorithm equivalent to ours.

### D. Parametric family

In a digital quantum computer the Hilbert space dimension  $N = 2^n$  is exponential in the number of qubits  $n \in \mathbb{N}$  and the Hilbert space has a natural tensor product decomposition into two-dimensional factors  $\mathbb{C}^N = \mathbb{C}^{2^n} = (\mathbb{C}^2)^{\otimes n}$ . A parametric family of unitaries relevant to variational quantum algorithms consists of decompositions into products of  $L \geq 1$  non-commuting layers of unitaries. Specifically, assume that the variational parameter vector is of the form  $\theta = \theta_1 \oplus \dots \oplus \theta_L \in \mathbb{R}^d$  where  $\oplus$  denotes the direct sum (concatenation) and consider a unitary operator acting on  $n$  qubits of the following form

$$U_L(\theta) := V_L(\theta_L)W_L \dots V_1(\theta_1)W_1 , \quad (14)$$

where  $V_l(\theta_l)$  and  $W_l$  are parametric and non-parametric unitary operators, respectively. For later convenience, we introduce the following notation for representing subcircuits between layers  $l_1 \leq l_2$

$$U_{[l_1:l_2]} := V_{l_2}W_{l_2} \dots V_{l_1}W_{l_1} , \quad (15)$$

so that, for example

$$U_L(\theta) = U_{(l:L)}V_lW_lU_{[1:l]} , \quad (16)$$

where  $(l : L) = [l - 1 : L]$  and  $[1 : l] = [1 : l - 1]$ . Moreover, we define the following convenience state for each layer  $l \in [L]$ :

$$\psi_l := U_{[1:l]}|0\rangle . \quad (17)$$

### E. Quantum Circuit Representation of Quantum Geometric Tensor

Computing the Quantum Geometric Tensor corresponding to a parametrized quantum circuit of the form (14) is a challenging task. In this section we will show, nevertheless, that block-diagonal components of the tensor can be efficiently computed on a quantum computer,

producing an approximation to the QGT of the following block-diagonal form:

$$\begin{matrix} & \boldsymbol{\theta}_1 & \boldsymbol{\theta}_2 & \cdots & \boldsymbol{\theta}_L \\ \boldsymbol{\theta}_1 & \boxed{G^{(1)}} & \mathbf{0} & \cdots & \mathbf{0} \\ \boldsymbol{\theta}_2 & \mathbf{0} & \boxed{G^{(2)}} & \cdots & \mathbf{0} \\ \vdots & \vdots & \vdots & \ddots & \vdots \\ \boldsymbol{\theta}_L & \mathbf{0} & \mathbf{0} & \cdots & \boxed{G^{(L)}} \end{matrix} . \quad (18)$$

Consider the  $l$ th layer of the circuit parametrized by  $\boldsymbol{\theta}_l$  and let  $\partial_i$  and  $\partial_j$  denote the partial derivative operators acting with respect to any pair of components of  $\boldsymbol{\theta}_l$  (not necessarily distinct). For each layer  $l \in [L]$  there exist Hermitian generator matrices  $K_i$  and  $K_j$  such that,

$$\partial_i V_l(\boldsymbol{\theta}_l) = -iK_i V_l(\boldsymbol{\theta}_l) , \quad (19)$$

$$\partial_j V_l(\boldsymbol{\theta}_l) = -iK_j V_l(\boldsymbol{\theta}_l) , \quad (20)$$

where for simplicity we have dropped the layer index  $l$  from the Hermitian generator  $K_j$ , despite the fact that the generators can vary between layers. The commutativity of the partial derivative operators combined with unitarity of  $V_l(\boldsymbol{\theta}_l)$  implies that  $[K_i, K_j] = 0$ .

Using (16), (19) and (20) we compute

$$\partial_j U_L(\boldsymbol{\theta}) = U_{(l:L)} \partial_j V_l(\boldsymbol{\theta}_l) W_l U_{[1:l]} , \quad (21)$$

$$= U_{(l:L)} (-iK_j) V_l(\boldsymbol{\theta}_l) W_l U_{[1:l]} , \quad (22)$$

$$= U_{(l:L)} (-iK_j) U_{[1:l]} . \quad (23)$$

Similarly, we have

$$\partial_i U_L(\boldsymbol{\theta})^\dagger = U_{[1:l]}^\dagger (iK_i^\dagger) U_{(l:L)}^\dagger . \quad (24)$$

It follows from unitarity of the subcircuit  $U_{(l:L)}$  and Hermiticity of the generator  $K_i$  that

$$\langle \partial_i \psi_\theta | \partial_j \psi_\theta \rangle = \langle \psi_l | K_i K_j | \psi_l \rangle . \quad (25)$$

Similarly, the so-called Berry connection is given by

$$i \langle \psi_\theta | \partial_j \psi_\theta \rangle = \langle \psi_l | K_j | \psi_l \rangle . \quad (26)$$

Combining these expressions we obtain the following form for the  $l$ th block of the QGT,

$$G_{ij}^{(l)} = \langle \psi_l | K_i K_j | \psi_l \rangle - \langle \psi_l | K_i | \psi_l \rangle \langle \psi_l | K_j | \psi_l \rangle . \quad (27)$$

The operator  $K_i K_j$  is Hermitian since  $[K_i, K_j] = 0$  and thus the block-diagonal approximation of the QGT coincides with the block-diagonal approximation of the Fubini-Study metric tensor,

$$g_{ij}^{(l)} = \text{Re}[G_{ij}^{(l)}] = G_{ij}^{(l)} . \quad (28)$$

The preceding calculation demonstrates the following key facts:

1. The  $l$ th block of the Fubini-Study metric tensor can be evaluated in terms of quantum expectation values of Hermitian observables.
2. The states  $\psi_l$  defining the quantum expectation values are prepared by subcircuits of the full quantum circuit and are thus experimentally realizable.

## F. Observables

Having identified the states for which the quantum expectation values are to be evaluated, we now turn to characterizing the Hermitian observables defining the quantum measurement.

For simplicity of exposition we focus on one of the most common parametric families encountered in the literature, which consists of tensor products of single-qubit Pauli rotations,

$$V_l(\boldsymbol{\theta}_l) = \bigotimes_{k=1}^n R_{P_{l,k}}(\boldsymbol{\theta}_{l,k}) . \quad (29)$$

The rotation gates are given by

$$R_{P_{l,k}}(\boldsymbol{\theta}_{l,k}) = \exp \left[ -i \frac{\boldsymbol{\theta}_{l,k}}{2} P_{l,k} \right] , \quad (30)$$

where  $\boldsymbol{\theta}_{l,k} \in [0, 2\pi)$ , and  $P_{l,k} \in \{\sigma_x, \sigma_y, \sigma_z\}$  denotes the Pauli matrix which acts on qubit  $k$  of layer  $l$ . The expressive power of this class of circuits was recently investigated in [25]. In this case the generators are easily shown to be

$$K_i = \frac{1}{2} \mathbb{1}^{[1,i]} \otimes P_{l,i} \otimes \mathbb{1}^{(i,n)} , \quad (31)$$

where  $\mathbb{1}^{[1,i]} = \bigotimes_{1 \leq j < i} \mathbb{1}$ . These operators evidently satisfy  $[K_i, K_j] = 0$ . Since  $P_{l,i}^2 = \mathbb{1}$  as a result of the Pauli algebra, it follows that the  $l$ th block of the QGT requires the evaluation of the quantum expectation value  $\langle \psi_l | \hat{A} | \psi_l \rangle$  where  $\hat{A} \in S_l$  belongs to the following set of operators

$$S_l = \{P_{l,i} \mid 1 \leq i \leq n\} \cup \{P_{l,i} P_{l,j} \mid 1 \leq i < j \leq n\} . \quad (32)$$

Furthermore, since every operator in  $S_l$  commutes, this implies that the number of state preparations is reduced from the naive counting  $|S_l| = n(n+1)/2$  to just a single measurement.

## III. NUMERICAL EXPERIMENTS

In order to validate the choice of geometry, numerical experiments were conducted to compare the Quantum Natural Gradient approach against vanilla gradient descent and the Adam optimizer. These experiments were performed with the open-source quantum machine learning software library PennyLane [9, 26]. New functionality was added for efficiently computing the block-diagonal  $g_{ij}^{(l)}$  and diagonal  $g_{ii}$  approximations of the Fubini-Study metric tensor for arbitrary  $n$ -qubit parametrized quantum circuits on quantum hardware.

This process involves the following steps:

1. **Represent the circuit as a directed acyclic graph (DAG).** This allows the parametrized layer structure to be programmatically extracted.

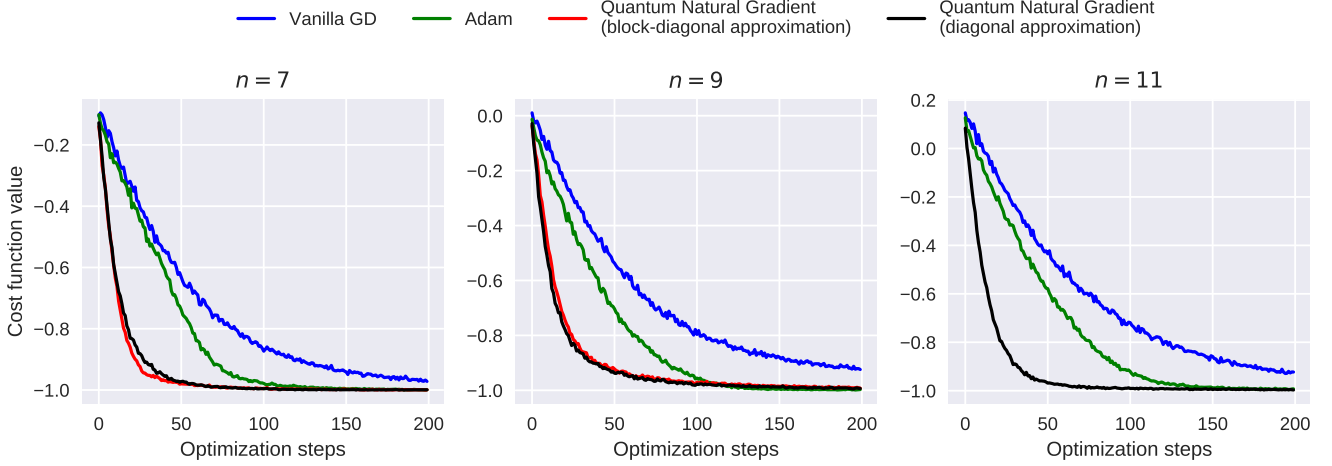


FIG. 1. The cost function value for  $n = 7, 9, 11$  qubits and  $l = 5$  layers as a function of training iteration for four different optimization dynamics. 8192 shots (samples) are used per required expectation value during optimization.

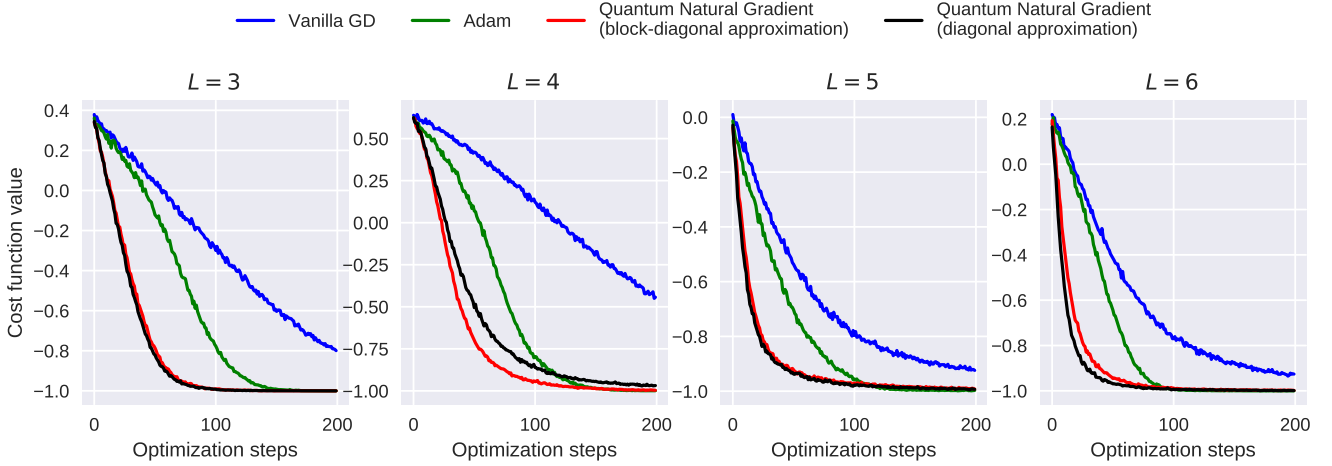


FIG. 2. The cost function value for  $n = 9$  qubits and  $l = 3, 4, 5, 6$  layers as a function of training iteration for four different optimization dynamics. 8192 shots (samples) are used per required expectation value during optimization.

Gates which have no dependence on each other (e.g., because they act on different wires) can be grouped together into the same layer.

2. **Determine observables.** For each layer  $l$  consisting of  $m$  parameters, the generators  $K_i$  for each parametrized gate are determined, and a subcircuit preparing  $\psi_l$  constructed.

3. **Calculate the  $l$ th block of the Fubini-Study metric tensor.**

- (a) **Entire block:** The unitary operation which rotates  $\psi_l$  into the shared eigenbasis of  $\{K_i | 1 \leq i \leq m\} \cup \{K_i K_j | 1 \leq i, j \leq m\}$  is calculated and applied to the subcircuit, and all qubits measured in the Pauli-Z basis. Classical post-processing is performed to determine

$\langle \psi_l | K_i K_j | \psi_l \rangle$ ,  $\langle \psi_l | K_i | \psi_l \rangle$ , and  $\langle \psi_l | K_j | \psi_l \rangle$  for all  $1 \leq i, j \leq m$ , and subsequently  $g_{ij}^{(l)}$ .

- (b) **Diagonal approximation:** The variance  $\langle K_i^2 \rangle - \langle K_i \rangle^2$  is computed for all  $1 \leq i \leq m$ , and subsequently the diagonal approximation to the block-diagonal,  $g_{ii}^{(l)}$ .

Thus, to evaluate the block-diagonal approximation of the Fubini-Study metric tensor on quantum hardware, a single quantum evaluation is performed for each layer in the parametrized quantum circuit. Finally, a Quantum Natural Gradient optimizer was implemented in PennyLane. This optimizer computes the pseudo-inverse of the block-diagonal metric tensor  $g^+(\theta)$  at each optimization step ( $L$  quantum evaluations), as well as the analytic gradient of the objective function  $\nabla \mathcal{L}(\theta)$  via the parameter shift rule ( $2d$  quantum evaluations),

and updates the parameter values via Eq. (13). As a result, each optimization step requires  $2d + L$  quantum evaluations.

For numerical verification, we considered the circuit of [27], which consists of an initial fixed layer of  $R_y(\pi/4)$  gates acting on  $n$  qubits, followed by  $L$  layers of parametrized Pauli rotations interwoven with 1D ladders of controlled-Z gates, and target Hermitian observable chosen to be the same two-Pauli operator  $Z_1 Z_2$  acting on the first and second qubit which has a ground state energy of  $-1$ . Starting from the same random initialization of Ref. [27], we optimize the parametrized Pauli rotation gates using vanilla gradient descent, the Adam optimizer, and the Quantum Natural Gradient optimizer, with both the block-diagonal and diagonal approximations. The results are shown in Fig. 1 for  $n = 7, 9, 11$  qubits,  $L = 5$  layers, and with the optimization performed using 8192 samples per expectation value. In all cases the vanilla gradient descent fails to find the minimum of the objective function, while the Quantum Natural Gradient descent finds the minimum in a small number of iterations, in both block-diagonal and strictly diagonal approximation. In addition, we present a comparison with the Adam optimizer which is a non-local averaging method. In this particular circuit, Adam is capable of finding the minimum but requires a larger number of iterations than the Quantum Natural Gradient. Furthermore, the improvement afforded by the Quantum Natural Gradient optimizer appears more significant with increasing qubit number. Note that for  $n = 11$ , we do not include the block-diagonal approximation, due to the increased classical overhead associated with numerically computing the shared eigenbasis for each parametrized layer. However, this overhead

can likely be negated by implementing the techniques of Crawford *et al.* [28] and Gokhale *et al.* [29].

To investigate the effects of variable circuit depth, the numerical experiment was repeated with  $n = 9$  qubits, and parametric quantum circuits with  $L = 3, 4, 5, 6$  layers. The results are shown in Fig. 2, highlighting that the Quantum Natural Gradient optimizer retains its advantage with increasing circuit depth.

#### IV. DISCUSSION

It is instructive to compare our proposal with existing preconditioning schemes such as Adam. Unlike Adam, which involves some kind of historical averaging, the preconditioning matrix suggested by quantum information geometry does not depend on the specific choice of loss function (Hermitian observable). It is instead a reflection of the local geometry of the quantum state space. In view of these differences it is natural to expect that the benefits provided by the Quantum Natural Gradient are complementary to those of existing stochastic optimization methods such as Adam. It is therefore of interest to perform a detailed ablative study combining these methods, which we leave to future work.

Finally, this paper only considered the relevant geometry for idealized systems described by pure quantum states. In near-term noisy devices it may be of interest to study the relevant geometry for density matrices. The most promising candidate is the Bures metric, which possesses a number of desirable features. In particular, it is the only monotone metric which reduces to both the Fubini-Study metric for pure states and the Fisher information matrix for classical mixtures [30].

#### Appendix A: Supplementary Material

In this appendix we employ the Einstein summation convention where summation over repeated indices is implied.

##### 1. Real and imaginary parts of Quantum Geometric Tensor

Partially differentiating both sides of the normalization condition  $1 = \|\psi_\theta\|^2$  with respect to  $\theta^i$  gives

$$\left\langle \psi_\theta, \frac{\partial \psi_\theta}{\partial \theta^i} \right\rangle + \left\langle \frac{\partial \psi_\theta}{\partial \theta^i}, \psi_\theta \right\rangle = 0 . \quad (\text{A1})$$

Partially differentiating again with respect to  $\theta^j$  gives

$$\left\langle \psi_\theta, \frac{\partial^2 \psi_\theta}{\partial \theta^i \partial \theta^j} \right\rangle + \left\langle \frac{\partial^2 \psi_\theta}{\partial \theta^i \partial \theta^j}, \psi_\theta \right\rangle + \left\langle \frac{\partial \psi_\theta}{\partial \theta^i}, \frac{\partial \psi_\theta}{\partial \theta^j} \right\rangle + \left\langle \frac{\partial \psi_\theta}{\partial \theta^j}, \frac{\partial \psi_\theta}{\partial \theta^i} \right\rangle = 0 . \quad (\text{A2})$$

Consider the wavefunction in a neighborhood  $\theta + \delta\theta$  of  $\theta \in \mathbb{R}^d$ . Taylor expanding in the displacement vector  $\delta\theta$  we obtain,

$$\psi_{\theta+\delta\theta} = \psi_\theta + \frac{\partial \psi_\theta}{\partial \theta^i} \delta\theta^i + \frac{1}{2} \frac{\partial^2 \psi_\theta}{\partial \theta^i \partial \theta^j} \delta\theta^i \delta\theta^j + \dots . \quad (\text{A3})$$

Taking the inner product with  $\psi_\theta$  gives

$$\langle \psi_\theta, \psi_{\theta+\delta\theta} \rangle = 1 + \left\langle \psi_\theta, \frac{\partial \psi_\theta}{\partial \theta^i} \right\rangle \delta\theta^i + \frac{1}{2} \left\langle \psi_\theta, \frac{\partial^2 \psi_\theta}{\partial \theta^i \partial \theta^j} \right\rangle \delta\theta^i \delta\theta^j + \dots \quad (\text{A4})$$

It follows that the fidelity between  $\psi_\theta$  and  $\psi_{\theta+\delta\theta}$  is given to quadratic order in the displacement  $\delta\theta$  by,

$$|\langle \psi_\theta, \psi_{\theta+\delta\theta} \rangle|^2 = \langle \psi_\theta, \psi_{\theta+\delta\theta} \rangle \langle \psi_{\theta+\delta\theta}, \psi_\theta \rangle \quad (\text{A5})$$

$$\begin{aligned} &= 1 + \left[ \left\langle \psi_\theta, \frac{\partial \psi_\theta}{\partial \theta^i} \right\rangle + \left\langle \frac{\partial \psi_\theta}{\partial \theta^i}, \psi_\theta \right\rangle \right] \delta\theta^i + \left[ \left\langle \frac{\partial \psi_\theta}{\partial \theta^i}, \psi_\theta \right\rangle \left\langle \psi_\theta, \frac{\partial \psi_\theta}{\partial \theta^j} \right\rangle + \frac{1}{2} \left\langle \psi_\theta, \frac{\partial^2 \psi_\theta}{\partial \theta^i \partial \theta^j} \right\rangle + \frac{1}{2} \left\langle \frac{\partial^2 \psi_\theta}{\partial \theta^i \partial \theta^j}, \psi_\theta \right\rangle \right] \delta\theta^i \delta\theta^j + \dots, \\ &= 1 + \left[ \left\langle \frac{\partial \psi_\theta}{\partial \theta^i}, \psi_\theta \right\rangle \left\langle \psi_\theta, \frac{\partial \psi_\theta}{\partial \theta^j} \right\rangle - \frac{1}{2} \left( \left\langle \frac{\partial \psi_\theta}{\partial \theta^i}, \frac{\partial \psi_\theta}{\partial \theta^j} \right\rangle + \left\langle \frac{\partial \psi_\theta}{\partial \theta^j}, \frac{\partial \psi_\theta}{\partial \theta^i} \right\rangle \right) \right] \delta\theta^i \delta\theta^j + \dots, \end{aligned} \quad (\text{A6})$$

where we have used (A1) and (A2). Now use the approximation

$$d^2(P_\psi, P_\phi) = \arccos^2(|\langle \psi, \phi \rangle|) = 1 - |\langle \psi, \phi \rangle|^2 + O((1 - |\langle \psi, \phi \rangle|^2)^2) \quad (\text{A7})$$

It follows that the infinitesimal squared distance is given by,

$$d^2(P_{\psi_\theta}, P_{\psi_{\theta+d\theta}}) = \left[ \frac{1}{2} \left( \left\langle \frac{\partial \psi_\theta}{\partial \theta^i}, \frac{\partial \psi_\theta}{\partial \theta^j} \right\rangle + \left\langle \frac{\partial \psi_\theta}{\partial \theta^j}, \frac{\partial \psi_\theta}{\partial \theta^i} \right\rangle \right) - \left\langle \frac{\partial \psi_\theta}{\partial \theta^i}, \psi_\theta \right\rangle \left\langle \psi_\theta, \frac{\partial \psi_\theta}{\partial \theta^j} \right\rangle \right] d\theta^i d\theta^j \quad (\text{A8})$$

The term multiplying  $\frac{1}{2}$  on the right-hand side of (A8) is manifestly real. The term multiplying  $-1$  is also real because of (A1) which implies

$$\text{Re} \left[ \left\langle \psi_\theta, \frac{\partial \psi_\theta}{\partial \theta^i} \right\rangle \right] = 0 \quad (\text{A9})$$

It follows that the metric tensor is given by the real part of the QGT,

$$d^2(P_{\psi_\theta}, P_{\psi_{\theta+d\theta}}) = \text{Re} \left[ \left\langle \frac{\partial \psi_\theta}{\partial \theta^i}, \frac{\partial \psi_\theta}{\partial \theta^j} \right\rangle - \left\langle \frac{\partial \psi_\theta}{\partial \theta^i}, \psi_\theta \right\rangle \left\langle \psi_\theta, \frac{\partial \psi_\theta}{\partial \theta^j} \right\rangle \right] d\theta^i d\theta^j \quad (\text{A10})$$

$$= \text{Re} [G_{ij}(\theta)] d\theta^i d\theta^j \quad (\text{A11})$$

For completeness, the imaginary part of the QGT is given by

$$\text{Im}[G_{ij}(\theta)] = -\frac{1}{2} \left[ \frac{\partial}{\partial \theta^i} A_j(\theta) - \frac{\partial}{\partial \theta^j} A_i(\theta) \right] \quad (\text{A12})$$

where  $A_i(\theta)$  is the Berry connection,

$$A_i(\theta) = i \left\langle \psi_\theta, \frac{\partial \psi_\theta}{\partial \theta^i} \right\rangle \quad (\text{A13})$$

## 2. Relationship with imaginary-time evolution

Consider the imaginary-time evolution operator  $e^{-H\delta\tau}$  generated by the Hermitian operator  $H$  where  $\delta\tau \in \mathbb{R}$ . Let  $P_{\psi_\theta} = |\psi_\theta\rangle\langle\psi_\theta|$  denote the projector onto the one-dimensional subspace spanned by the unit vector  $\psi_\theta$  and let  $\bar{\psi}_\theta = e^{-H\delta\tau}\psi_\theta$ . Then the projected imaginary-time evolution is defined by,

$$\arg \min_{\delta\theta \in \mathbb{R}^d} \|\bar{\psi}_\theta - P_{\psi_{\theta+\delta\theta}} \bar{\psi}_\theta\|^2 = \arg \max_{\delta\theta \in \mathbb{R}^d} |\langle \bar{\psi}_\theta, \psi_{\theta+\delta\theta} \rangle|^2 \quad (\text{A14})$$

where we used the normalization of  $\psi_{\theta+\delta\theta}$ . We have

$$\langle \bar{\psi}_\theta, \psi_{\theta+\delta\theta} \rangle = \langle \bar{\psi}_\theta, \psi_\theta \rangle + \left\langle \bar{\psi}_\theta, \frac{\partial \psi_\theta}{\partial \theta^i} \right\rangle \delta\theta^i + \frac{1}{2} \left\langle \bar{\psi}_\theta, \frac{\partial^2 \psi_\theta}{\partial \theta^i \partial \theta^j} \right\rangle \delta\theta^i \delta\theta^j + \dots \quad (\text{A15})$$

So Taylor expanding  $|\langle \bar{\psi}_\theta, \psi_{\theta+\delta\theta} \rangle|^2$  to quadratic order in the displacement gives,

$$\begin{aligned} |\langle \bar{\psi}_\theta, \psi_{\theta+\delta\theta} \rangle|^2 &= |\langle \bar{\psi}_\theta, \psi_\theta \rangle|^2 + \left[ \langle \psi_\theta, \bar{\psi}_\theta \rangle \left\langle \bar{\psi}_\theta, \frac{\partial \psi_\theta}{\partial \theta^i} \right\rangle + \left\langle \frac{\partial \psi_\theta}{\partial \theta^i}, \bar{\psi}_\theta \right\rangle \langle \bar{\psi}_\theta, \psi_\theta \rangle \right] \delta\theta^i + \\ &+ \left[ \left\langle \frac{\partial \psi_\theta}{\partial \theta^i}, \bar{\psi}_\theta \right\rangle \left\langle \bar{\psi}_\theta, \frac{\partial \psi_\theta}{\partial \theta^j} \right\rangle + \frac{1}{2} \langle \psi_\theta, \bar{\psi}_\theta \rangle \left\langle \bar{\psi}_\theta, \frac{\partial^2 \psi_\theta}{\partial \theta^i \partial \theta^j} \right\rangle + \frac{1}{2} \left\langle \frac{\partial^2 \psi_\theta}{\partial \theta^i \partial \theta^j}, \bar{\psi}_\theta \right\rangle \langle \bar{\psi}_\theta, \psi_\theta \rangle \right] \delta\theta^i \delta\theta^j + \dots \end{aligned} \quad (\text{A16})$$

Expanding the exponential  $e^{-H\delta\tau}$  in  $\delta\tau$  and neglecting cubic-order terms in the multi-variable Taylor expansion in  $\delta\theta$  and  $\delta\tau$ ,

$$|\langle \bar{\psi}_\theta, \psi_{\theta+\delta\theta} \rangle|^2 = |\langle \bar{\psi}_\theta, \psi_\theta \rangle|^2 - \left[ \left\langle \frac{\partial \psi_\theta}{\partial \theta^i}, H\psi_\theta \right\rangle + \left\langle H\psi_\theta, \frac{\partial \psi_\theta}{\partial \theta^i} \right\rangle \right] \delta\theta^i \delta\tau - \text{Re}[G_{ij}(\theta)] \delta\theta^i \delta\theta^j + \dots, \quad (\text{A17})$$

where we have made use of (A1) and (A2). The first-order optimality condition  $0 = \frac{\partial}{\partial \delta\theta^i} |\langle \bar{\psi}_\theta, \psi_{\theta+\delta\theta} \rangle|^2$ , at lowest order in  $\delta\theta$  and  $\delta\tau$ , thus gives

$$0 = - \left[ \left\langle \frac{\partial \psi_\theta}{\partial \theta^i}, H\psi_\theta \right\rangle + \left\langle H\psi_\theta, \frac{\partial \psi_\theta}{\partial \theta^i} \right\rangle \right] \delta\tau - 2 \text{Re}[G_{ij}(\theta)] \delta\theta^j + \dots, \quad (\text{A18})$$

$$= -\frac{1}{2} \left[ \left\langle \frac{\partial \psi_\theta}{\partial \theta^i}, H\psi_\theta \right\rangle + \left\langle \psi_\theta, H \frac{\partial \psi_\theta}{\partial \theta^i} \right\rangle \right] \delta\tau - \text{Re}[G_{ij}(\theta)] \delta\theta^j \dots, \quad (\text{A19})$$

$$= -\frac{\partial}{\partial \theta^i} \mathcal{L}(\theta) \delta\tau - \text{Re}[G_{ij}(\theta)] \delta\theta^j + \dots, \quad (\text{A20})$$

where  $\mathcal{L}(\theta) = \frac{1}{2} \langle \psi_\theta, H\psi_\theta \rangle$  and we have used  $H = H^\dagger$ . In the limit  $\delta\tau \rightarrow 0$  we obtain the following system of ordinary differential equations,

$$g(\theta(\tau)) \dot{\theta}(\tau) = -\nabla \mathcal{L}(\theta(\tau)). \quad (\text{A21})$$

### 3. Relationship with classical Fisher information

Let  $\{|x\rangle : x \in [N]\}$  be an orthonormal basis for  $\mathbb{C}^N$  and suppose  $p_\theta(x)$  is a parametric family of probability distributions on the finite set  $[N]$ . Define the following parametric family of quantum states

$$\psi_\theta = \sum_{x \in [N]} \sqrt{p_\theta(x)} |x\rangle. \quad (\text{A22})$$

Then by the chain rule

$$\frac{\partial \psi_\theta}{\partial \theta^i} = \frac{1}{2} \sum_{x \in [N]} \frac{1}{\sqrt{p_\theta(x)}} \frac{\partial p_\theta(x)}{\partial \theta^i} |x\rangle. \quad (\text{A23})$$

Thus the Berry connection for this family of states vanishes

$$\left\langle \psi_\theta, \frac{\partial \psi_\theta}{\partial \theta^i} \right\rangle = \frac{1}{2} \sum_{x \in [N]} \sum_{x' \in [N]} \frac{\sqrt{p_\theta(x')}}{\sqrt{p_\theta(x)}} \frac{\partial p_\theta(x)}{\partial \theta^i} \langle x' | x \rangle, \quad (\text{A24})$$

$$= \frac{1}{2} \sum_{x \in [N]} \frac{\partial p_\theta(x)}{\partial \theta^i}, \quad (\text{A25})$$

$$= \frac{1}{2} \frac{\partial}{\partial \theta^i} \sum_{x \in [N]} p_\theta(x), \quad (\text{A26})$$

$$= \frac{1}{2} \frac{\partial}{\partial \theta^i} 1, \quad (\text{A27})$$

$$= 0, \quad (\text{A28})$$



where we used the orthonormality of the basis  $\langle x'|x \rangle = \delta_{xx'}$ . The QGT is thus given by

$$G_{ij}(\theta) = \left\langle \frac{\partial \psi_\theta}{\partial \theta^i}, \frac{\partial \psi_\theta}{\partial \theta^j} \right\rangle, \quad (\text{A29})$$

$$= \frac{1}{4} \sum_{x \in [N]} \sum_{x' \in [N]} \frac{1}{\sqrt{p_\theta(x)p_\theta(x')}} \frac{\partial p_\theta(x)}{\partial \theta^i} \frac{\partial p_\theta(x')}{\partial \theta^j} \langle x'|x \rangle, \quad (\text{A30})$$

$$= \frac{1}{4} \sum_{x \in [N]} \frac{1}{p_\theta(x)} \frac{\partial p_\theta(x)}{\partial \theta^i} \frac{\partial p_\theta(x)}{\partial \theta^j}, \quad (\text{A31})$$

$$= \frac{1}{4} \sum_{x \in [N]} p_\theta(x) \frac{\partial \log p_\theta(x)}{\partial \theta^i} \frac{\partial \log p_\theta(x)}{\partial \theta^j}, \quad (\text{A32})$$

$$= \frac{1}{4} I_{ij}(\theta). \quad (\text{A33})$$

- [1] J. Preskill, *Quantum* **2**, 79 (2018).
- [2] A. Peruzzo, J. McClean, P. Shadbolt, M.-H. Yung, X.-Q. Zhou, P. J. Love, A. Aspuru-Guzik, and J. L. O'Brien, *Nature Communications* **5**, 4213 (2014).
- [3] E. Farhi, J. Goldstone, and S. Gutmann, arXiv preprint arXiv:1411.4028 (2014).
- [4] E. Farhi and H. Neven, arXiv preprint arXiv:1802.06002 (2018).
- [5] W. J. Huggins, P. Patil, B. Mitchell, K. B. Whaley, and M. Stoudenmire, *Quantum Science and Technology* **4**, 024001 (2018).
- [6] M. Schuld, A. Bocharov, K. Svore, and N. Wiebe, arXiv preprint arXiv:1804.00633 (2018).
- [7] G. G. Guerreschi and M. Smelyanskiy, arXiv preprint arXiv:1701.01450 (2017).
- [8] J. C. Spall *et al.*, *IEEE Transactions on Automatic Control* **37**, 332 (1992).
- [9] M. Schuld, V. Bergholm, C. Gogolin, J. Izaac, and N. Killoran, *Physical Review A* **99**, 032331 (2019).
- [10] S. Jastrzebski, Z. Kenton, D. Arpit, N. Ballas, A. Fischer, Y. Bengio, and A. Storkey, arXiv preprint arXiv:1711.04623 (2017).
- [11] D. P. Kingma and J. Ba, arXiv preprint arXiv:1412.6980 (2014).
- [12] B. Neyshabur, R. R. Salakhutdinov, and N. Srebro, in *Advances in Neural Information Processing Systems* (2015) pp. 2422–2430.
- [13] S.-I. Amari, *Neural Computation* **10**, 251 (1998).
- [14] T. Liang, T. Poggio, A. Rakhlin, and J. Stokes, arXiv preprint arXiv:1711.01530 (2017).
- [15] A. Harrow and J. Napp, arXiv preprint arXiv:1901.05374 (2019).
- [16] F. Wilczek and A. Shapere, *Geometric Phases In Physics*. Series: Advanced Series in Mathematical Physics, ISBN: 978-9971-5-0621-6. WORLD SCIENTIFIC, Edited by F Wilczek and A Shapere, vol. 5 **5** (1989).
- [17] S. Sorella, M. Casula, and D. Rocca, *The Journal of Chemical Physics* **127**, 014105 (2007).
- [18] Y. Li and S. C. Benjamin, *Physical Review X* **7**, 021050 (2017).
- [19] M.-C. Chen, M. Gong, X.-S. Xu, X. Yuan, J.-W. Wang, C. Wang, C. Ying, J. Lin, Y. Xu, Y. Wu, *et al.*, arXiv preprint arXiv:1905.03150 (2019).
- [20] P. Kramer and M. Saraceno, *Geometry of the time-dependent variational principle in quantum mechanics* (Springer, 1981).
- [21] S. McArdle, T. Jones, S. Endo, Y. Li, S. C. Benjamin, and X. Yuan, *npj Quantum Information* **5**, 1 (2019).
- [22] T. Jones and S. C. Benjamin, arXiv preprint arXiv:1811.03147 (2018).
- [23] T. Jones, S. Endo, S. McArdle, X. Yuan, and S. C. Benjamin, *Physical Review A* **99**, 062304 (2019).
- [24] X. Yuan, S. Endo, Q. Zhao, Y. Li, and S. C. Benjamin, *Quantum* **3**, 191 (2019).
- [25] Y. Du, M.-H. Hsieh, T. Liu, and D. Tao, arXiv preprint arXiv:1810.11922 (2018).
- [26] V. Bergholm, J. Izaac, M. Schuld, C. Gogolin, and N. Killoran, arXiv preprint arXiv:1811.04968 (2018).
- [27] J. R. McClean, S. Boixo, V. N. Smelyanskiy, R. Babbush, and H. Neven, *Nature communications* **9**, 4812 (2018).
- [28] O. Crawford, B. van Straaten, D. Wang, T. Parks, E. Campbell, and S. Brierley, arXiv preprint arXiv:1908.06942 (2019).
- [29] P. Gokhale, O. Angiuli, Y. Ding, K. Gui, T. Tomesh, M. Suchara, M. Martonosi, and F. T. Chong, arXiv preprint arXiv:1907.13623 (2019).
- [30] D. Petz, in *Quantum Probability Communications: Volume X* (World Scientific, 1998) pp. 135–157.